Mével, C., Gillis, K.M., Allan, J.F., and Meyer, P.S. (Eds.), 1996
Proceedings of the Ocean Drilling Program, Scientific Results, Vol. 147

27. DETRITAL MINERALS IN SURFACE SEDIMENTS FROM HESS DEEP, EQUATORIAL PACIFIC: IMPLICATIONS FOR THE LITHOLOGIC SPREAD OF MAFIC-ULTRAMAFIC ROCKS[1]

Shoji Arai[2] and Natsue Abe[2]

ABSTRACT

Surface sediments from Holes 894D, 894E, and 895A of ODP Leg 147 were examined for chromian spinel and other detrital minerals in order to determine the source rocks of the Hess Deep sediments. The detrital chromian spinel, except for that in basalt particles, has an intermediate Cr# (= Cr/[Cr + Al] atomic ratio), similar to spinel in ultramafic-mafic plutonic rocks drilled at Site 895. Chromian spinel derived from peridotites and related mafic plutonic rocks was not found in sediments from Site 894. Detrital spinel from Site 895 is generally low in Ti, which indicates a derivation mainly from harzburgite or peridotite intermediate between harzburgite and dunite, that is, a slightly melt-impregnated harzburgite. The peridotites that supplied the clastic particles represent less melt-impregnated rocks than the peridotites cored at Site 895. Lherzolitic peridotites, which have chromian spinel with Cr# <0.4 and are predominant in the Atlantic fracture zones, are absent in Hess Deep.

INTRODUCTION

Some serpentinite breccias or sandstones form near serpentinite exposures or cliffs in the ocean floor, especially at oceanic fracture zones (e.g., Bonatti et al., 1973, 1974). Some detrital minerals, especially chromian spinel and clinopyroxene, in sediments can be a good petrographic indicator of the source rocks (e.g., Arai et al., 1983; Arai and Okada, 1991). These minerals can provide information on the spatial lithologic variation of presently exposed rocks or on the lithology of rocks lost by erosion. The chemical composition of chromian spinel is affected by the physicochemical conditions of its crystallization and is a good petrogenetic indicator for mafic-ultramafic rocks (Irvine, 1967; Jackson, 1969; Evans and Frost, 1975; Dick and Bullen, 1984; Arai, 1992).

During Ocean Drilling Program (ODP) Leg 147, mafic and ultramafic plutonic rocks were recovered from Sites 894 and 895, at Hess Deep in the equatorial Pacific. Submersible surveys indicate that gabbroic rocks (both cumulate and noncumulate) and, less commonly, basaltic rocks are exposed around Site 894 (Francheteau et al., 1990). On the other hand, both peridotites (harzburgite and dunite) and cumulate gabbros are exposed around Site 895 (Francheteau et al., 1990, 1992). Drilling results from Leg 147 are consistent with the submersible observations. Gabbroic rocks and ultramafic rocks were obtained mostly from Sites 894 and 895, respectively (Gillis, Mével, Allan, et al., 1993). No ultramafic rocks were cored at Site 894. The cores from Site 895 are dominated by ultramafic rocks with intervening gabbroic and troctolitic rocks; harzburgite is predominant over dunite in core from Hole 895D and vice versa in core from Hole 895E (Gillis, Mével, Allan, et al., 1993).

Drilling through the ocean floor clarifies the vertical lithologic variation at each hole. The petrography of the surface sediments may provide information on the spatial lithologic variation for exposed rocks, if any. Some detrital minerals, including chromian spinel, in the surface sediments obtained from Holes 894D, 894E, and 895A were examined in order to estimate the lithologic spread of the exposed rocks around each site.

PETROGRAPHY OF THE SEDIMENTS

Hole 894D

Sample 147-894D-1R-1, 129–130 cm, was examined. The sediments are composed of subangular to rounded, fine- to medium-grained sand particles of mafic effusive rocks with abundant calcareous materials. Basaltic particles are typically glassy and aphyric and brown in thin section. Fine-grained basalt with acicular plagioclase was also found. Olivine is prominent as a detrital mineral grain.

Olivine, plagioclase, hornblende, and augite were found as detrital mineral particles. Olivine is clear and has rare, small, euhedral chromian spinel inclusions. Plagioclase is usually turbid, and some of the hornblende includes olivine.

Hole 894E

The sediments of Sample 147-894E-1R-2, 66–67 cm, are dominated by calcareous materials and small amounts of basalt particles. The clastic particles are poorly sorted and vary from very coarse sand to pebbles in size. They are extremely poor in detrital mineral grains, although olivine and turbid plagioclase were observed. Some of the basalt is glassy and some is fine grained, which is similar in appearance to that in the Hole 894D sediments. Sporadic olivine phenocrysts with euhedral chromian spinel inclusions were observed in the basalt pebbles (Pl. 1, Fig. 1).

Hole 895A

Five samples (147-895A-1R-1, 10–12 cm, 22–24 cm, and 35–37 cm, and 147-895A-1R-2, 31–33 cm, and 36–38 cm) were examined for their detrital mineralogy. These sediments are composed of poorly sorted lithic and mineral particles with fine-grained biogenic calcareous materials. The clastic particles vary in size from fine sand to pebbles. Subangular to subrounded particles of serpentinite with a mesh structure, which formed subsequent to the olivine, are abundant (Pl. 1, Fig. 2). Angular particles of fibrous chrysotile serpentine, which commonly form veinlets in serpentinized peridotites, are also prominent. Fine-grained or glassy basalts and dolerites were also

[1]Mével, C., Gillis, K.M., Allan, J.F., and Meyer, P.S. (Eds.), 1996. *Proc. ODP, Sci. Results,* 147: College Station, TX (Ocean Drilling Program).
[2]Department of Earth Sciences, Faculty of Science, Kanazawa University, Kakuma-machi, Kanazawa 920-11, Japan.

found as lithic particles. The mineral particles are more angular than the lithic ones.

The detrital minerals are composed of olivine, orthopyroxene, clinopyroxene, chromian spinel, plagioclase, and hornblende, irrespective of the depth of the sample in the Hole 895A core. Some of the chromian spinel is highly anhedral, possibly derived from harzburgite (Pl. 1, Fig. 3), and some is rounded, possibly derived from dunite (Pl. 1, Fig. 4). Chromian spinel is usually altered to magnetite or ferritchromite along cracks (Pl. 1, Figs. 3 and 4). Some of the olivine is turbid and is similar in appearance to the peridotite olivine.

MINERAL CHEMISTRY

Analytical Method

Minerals were analyzed using an Akashi Alpha30 SEM-EDAX system with an energy-dispersive spectrometer at Kanazawa University. The detection limit is approximately 0.1 wt% for major oxides except for Na_2O, for which it is approximately 0.3 wt%. The reproducibility of the data is sufficiently good for the major elements. The Mg# (= Mg/[Mg + total iron] atomic ratio) of the silicates and the Cr# (= Cr/[Cr + Al] atomic ratio) were determined with special care; these ratios are reproducible to about ±0.2% and about ±0.8%, respectively, on repeated runs.

Chromian Spinel

Compositions of chromian spinel are shown in Figures 1 through 3 and all analyses are listed in Table 1. Two types of detrital chromian spinel can be distinguished: (1) relatively small euhedra included in basaltic particles and (2) relatively coarse mineral particles commonly associated with serpentine. The former type of spinel was found only in the Site 894 sediments and the latter type of spinel was found only in the Site 895 sediments. As is normal for magmatic chromian spinels, the Mg# correlates negatively with the Cr# for all spinel grains examined (Fig. 1). The $Fe^{3+}/(Cr + Al + Fe^{3+})$ ratio is very low for both types of spinel (Fig. 2) and the TiO_2 content is relatively low, generally less than 1 wt% and commonly less than 0.5 wt% (Fig. 3). Both the Fe^{3+} ratio and the TiO_2 content are in the range of spinels in mid-ocean-ridge basalts (MORB) or ocean-floor peridotites (e.g., Dick and Bullen, 1984; Arai, 1992). The Cr# is not correlated with the TiO_2 content for spinels both from surface sediments and from cored rocks at Hess Deep (Fig. 3). The euhedral spinel in the basalt particles has a high Mg# (approximately 0.63) and a low Cr# (approximately 0.34). It is within the field of typical MORB spinels in terms of the Fe^{3+}-TiO_2 relation (Arai, 1992).

Silicates

Phenocryst olivine from Hole 894E, which coexists with chromian spinel with a Cr# = 0.34, is Fo_{88-89} in composition. Detrital olivine in the Hole 894D sediments ranges from Fo_{86} to Fo_{90} in composition. The magnesian olivine with Fo_{90} is also high in NiO (0.3 to 0.4 wt%) and in CaO (0.3 wt%). The olivine in the sediments from Hole 895A is generally magnesian, Fo_{90-91} in composition, high in NiO (0.3 to 0.4 wt%), and low in CaO (0.1 wt%).

Orthopyroxene is less common than olivine and is enstatite with a high Mg# (0.91). The clinopyroxene can be divided into two types in terms of chemistry (Fig. 4). One is augite with an intermediate Mg#, from 0.58 to 0.75, and low Cr_2O_3 contents, less than 0.3 wt%. The other is chrome diopside with 0.8–1.3 wt% Cr_2O_3 and a high Mg#, mostly 0.91–0.92.

Hornblende is relatively variable in its chemistry; the Mg# ranges from 0.44 to 0.64 and is negatively correlated with the TiO_2 content, from 2.3 to 1.0 wt%. Tremolitic amphibole with a very low Al_2O_3 content was also found.

Plagioclase is quite variable in composition, from An_{81} to An_2 and most commonly An_{50-60}.

DISCUSSION

All of the chromian spinel grains, except for the small euhedral ones in basaltic particles, may be derived from olivine-rich plutonic rocks, peridotites, troctolites, and olivine gabbros, as their chemical characteristics are very similar to those of chromian spinel in the drilled rocks (Arai and Matsukage, this volume). Also, the Cr# of spinel in peridotites and related mafic plutonic rocks exposed at Hess Deep is relatively constant, at about 0.5. The relatively low-Ti character of the detrital spinels indicates that their derivation is mainly from harzburgitic rocks (Fig. 3). This is consistent with the predominance of harzburgite over other rocks in Hole 895D, which is located close to Hole 895A from which the sediments were obtained (Gillis, Mével, Allan, et al., 1993). Chromian spinel in harzburgite from the drill cores is very low in TiO_2, less than 0.2 wt%. The detrital spinel with an intermediate TiO_2 content (0.2 to 0.5 wt%) is possibly derived from transitional rocks, from typical harzburgite to dunite, that is, the slightly melt-impregnated harzburgite according to the interpretation of Arai and Matsukage (this volume), who proposed the formation of a dunite-troctolite-olivine gabbro series by an interaction between harzburgite and impregnated melt.

It is noteworthy that lherzolitic peridotites with a Cr# of spinel lower than 0.5, which are common from the ocean floor (e.g., Dick and Bullen, 1984; Dick, 1989), are absent at Hess Deep. The oceanic lherzolites are derived mostly from the Atlantic and Indian Oceans, especially from their fracture zones (e.g., Bonatti and Hamlyn, 1978; Dick et al., 1984; Bonatti et al., 1992). The constant and high Cr# of spinel in harzburgite from Hess Deep strongly indicates that the melting conditions are different between the East Pacific Rise and the Mid-Atlantic or Mid-Indian Ocean Ridges. It is most probable that the degree of partial fusion or the degree of melt extraction at MORB genesis from a source peridotite is higher at the fast-spreading ridge system than at the slow-spreading one. It may be especially low in the neighborhood of fracture zones at the latter.

Hornblende and some olivine and plagioclase grains from the sediments from Hole 894D are coarse and are possibly derived from gabbroic rocks, although the shipboard description suggests that the sediments are composed mainly of basaltic sand (Gillis, Mével, Allan, et al., 1993). An olivine phenocryst in a basalt particle of the sediments from Hole 894E is magnesian (Fo_{88-89}) and coexists with chromian spinel with Cr# = 0.34. This indicates that the basalt is primitive, possible primary, and can coexist with a lherzolitic peridotite (Arai, 1994). Detrital olivine can be divided into two groups: low Ca (CaO 0.1 wt%) and high Ca (CaO 0.3 wt%) (Table 2). The former is high both in Fo (90–91) and in NiO (0.3 to 0.4 wt%) contents and is probably derived from peridotites. The latter may be derived from some basaltic rocks. Olivine in gabbroic rocks, which has a CaO content as low as peridotite olivine and has variable but low Fo and NiO contents (Arai and Matsukage, this volume), was not found in the surface sediments. Orthopyroxene, which has high a Mg# (0.91) in the Hole 895A sediments, is similar in chemistry and appearance to that in the cored harzburgite (Arai and Matsukage, this volume). Augite is possibly derived from gabbroic rocks because the basaltic rocks are too Mg rich, as deduced from the high Mg# of possible olivine phenocrysts (Fo_{88-90}) discussed above, to contain augite with an intermediate Mg# (0.58 to 0.75). Chrome diopside with a high Mg#, mostly 0.91–0.92, is derived from peridotites.

In summary, the detrital mineralogy is similar to the cored rock mineralogy. Therefore, it is probable that the detrital minerals from the Site 894 sediments are derived mostly from gabbroic rocks and those from the Hole 895 sediments from peridotites and gabbros.

Table 1. Electron microprobe analyses of the detrital chromian spinels from Hess Deep.

Hole:	894E		895A								
TiO_2	0.30	0.49	0.13	0.26	0.34	0.86	0.07	0.15	0.25	0.04	0.05
Al_2O_3	37.18	36.35	30.96	26.51	25.89	20.76	25.73	26.67	23.76	23.08	27.11
Cr_2O_3	29.13	29.79	36.18	42.08	42.50	44.87	42.08	41.03	41.66	41.47	40.84
FeO*	15.15	15.05	17.91	16.69	17.07	22.29	19.22	17.64	22.19	23.31	17.52
MnO	0.11	0.46	0.00	0.35	0.31	0.43	0.39	0.50	0.48	0.47	0.00
MgO	16.83	16.58	14.10	13.58	13.10	10.21	12.25	13.21	11.32	11.05	14.09
NiO	0.31	0.32	0.25	0.05	0.17	0.09	0.11	0.21	0.10	0.17	0.14
Total	99.02	99.05	99.52	99.53	99.38	99.51	99.86	99.41	99.75	99.58	99.75
Ti	0.007	0.011	0.003	0.006	0.008	0.021	0.002	0.004	0.006	0.001	0.001
Al	1.263	1.239	1.089	0.949	0.932	0.780	0.931	0.959	0.877	0.860	0.967
Cr	0.663	0.681	0.854	1.010	1.027	1.131	1.022	0.990	1.032	1.036	0.977
Fe*	0.365	0.364	0.447	0.424	0.436	0.594	0.494	0.450	0.581	0.616	0.443
Mn	0.003	0.011	0.000	0.009	0.008	0.012	0.010	0.013	0.013	0.013	0.000
Mg	0.723	0.715	0.627	0.615	0.597	0.485	0.561	0.601	0.529	0.521	0.635
Ni	0.007	0.008	0.006	0.001	0.004	0.002	0.003	0.005	0.003	0.004	0.003
Total	3.030	3.029	3.026	3.014	3.012	3.024	3.022	3.022	3.040	3.051	3.027
Mg#	0.723	0.720	0.625	0.618	0.602	0.494	0.560	0.602	0.527	0.515	0.631
Cr#	0.344	0.355	0.439	0.516	0.524	0.592	0.523	0.508	0.541	0.547	0.503
$Cr/(Cr + Al + Fe^{3+})$	0.332	0.343	0.425	0.507	0.517	0.575	0.510	0.496	0.515	0.513	0.485
$Al/(Cr + Al + Fe^{3+})$	0.631	0.624	0.543	0.477	0.470	0.397	0.465	0.481	0.438	0.425	0.480
$Fe^{3+}/(Cr + Al + Fe^{3+})$	0.037	0.033	0.032	0.016	0.013	0.028	0.025	0.023	0.048	0.062	0.035

Notes: Cation fractions calculated assuming spinel stoichiometry. All Ti assumed to form the ulvöspinel molecule, $Fe^{2+}{}_2TiO_4$. FeO* and Fe* indicate total iron as FeO and Fe, respectively. Mg# and Cr# are $Mg/(Mg + Fe^{2+})$ and $Cr/(Cr + Al)$ atomic ratios, respectively.

Hole:	895A (continued).									
TiO_2	0.01	0.12	0.72	0.10	0.32	0.10	0.02	0.00	0.23	0.21
Al_2O_3	25.49	29.60	26.71	24.76	25.63	24.42	29.05	26.45	25.79	26.01
Cr_2O_3	43.59	38.61	39.16	42.76	39.30	42.17	38.14	42.14	41.38	41.86
FeO*	16.43	17.04	19.05	18.78	22.76	19.75	19.01	16.59	18.71	17.66
MnO	0.00	0.00	0.00	0.54	0.53	0.55	0.55	0.44	0.75	0.54
MgO	14.08	14.28	13.87	12.27	11.09	12.35	12.37	13.48	12.36	13.08
NiO	0.18	0.22	0.24	0.19	0.00	0.12	0.09	0.18	0.17	0.28
Total	99.78	99.87	99.76	99.41	99.64	99.47	99.22	99.28	99.40	99.63
Ti	0.000	0.003	0.016	0.002	0.007	0.002	0.000	0.000	0.005	0.005
Al	0.913	1.041	0.957	0.903	0.941	0.894	1.041	0.950	0.936	0.937
Cr	1.047	0.911	0.941	1.046	0.968	1.035	0.917	1.016	1.008	1.011
Fe*	0.417	0.425	0.484	0.486	0.593	0.513	0.484	0.423	0.482	0.451
Mn	0.000	0.000	0.000	0.014	0.014	0.015	0.014	0.011	0.020	0.014
Mg	0.638	0.635	0.629	0.566	0.515	0.572	0.561	0.612	0.568	0.596
Ni	0.004	0.005	0.006	0.005	0.000	0.003	0.002	0.004	0.004	0.007
Total	3.020	3.021	3.034	3.023	3.038	3.033	3.020	3.017	3.023	3.021
Mg#	0.635	0.634	0.633	0.567	0.515	0.570	0.560	0.612	0.571	0.599
Cr#	0.534	0.467	0.496	0.537	0.507	0.537	0.468	0.517	0.518	0.519
$Cr/(Cr + Al + Fe^{3+})$	0.521	0.454	0.474	0.524	0.484	0.516	0.458	0.508	0.507	0.508
$Al/(Cr + Al + Fe^{3+})$	0.454	0.519	0.482	0.452	0.470	0.446	0.520	0.475	0.471	0.471
$Fe^{3+}/(Cr + Al + Fe^{3+})$	0.025	0.026	0.044	0.024	0.046	0.038	0.021	0.017	0.023	0.021

CONCLUSIONS

The sediments from Site 894 are derived from basalts and gabbros. Those from Site 895 are derived from peridotites and gabbros. The detrital chromian spinels are generally TiO_2 poor, which possibly indicates the predominance of harzburgite or the peridotite transitional from harzburgite to dunite (i.e., the slightly melt-impregnated harzburgite) in the mantle rocks exposed at Hess Deep. The peridotites that supplied the clastic materials are generally less melt impregnated than the cored peridotitic suites recovered during Leg 147. Lherzolitic peridotites, which are common in the Atlantic and Indian Oceans, are absent at Hess Deep.

ACKNOWLEDGMENTS

S.A. wishes to express his hearty appreciation to K. Gillis, C. Mével, J. Allan, other shipboard scientists, marine technicians, and the captain and crew of *JOIDES Resolution* during the Leg 147 cruise for their collaboration and hospitality. S.A. is greatly indebted to A. Taira for the trouble he took to send S.A. on the ODP cruise. We are grateful to K. Matsukage for her suggestions and discussion. Critical comments by J. Allan, M. Clynne, and G. Gaetani greatly helped improve the manuscript.

REFERENCES

Arai, S., 1992. Chemistry of chromian spinels in volcanic rocks as a potential guide to magma chemistry. *Mineral. Mag.*, 56:173–184.

————, 1994. Compositional variation of olivine-chromian spinel in Mg-rich magmas as a guide to their residual spinel peridotites. *J. Volcanol. Geotherm. Res.*, 59:279–293.

Arai, S., Ito, T., and Ozawa, K., 1983. Ultramafic-mafic clastic rocks from the Mineoka belt, central Japan. *Chishitsugaku Zasshi* [*J. Geol. Soc. Jpn.*], 89:287–297. (in Japanese with English abstract)

Arai, S., and Okada, H., 1991. Petrology of serpentine sandstone as a key to tectonic development of serpentine belts. *Tectonophysics,* 195:65–81.

Bonatti, E., Emiliani, C., Ferrara, G., Honnorez, J., and Rydell, H., 1974. Ultramafic-carbonate breccias from the equatorial Mid-Atlantic Ridge. *Mar. Geol.,* 16:83–102.

Bonatti, E., and Hamlyn, P.R., 1978. Mantle uplifted block in the western Indian Ocean. *Science,* 201:249–251.

Bonatti, E., Honnorez, J., and Gartner, S., Jr., 1973. Sedimentary serpentinites from the Mid-Atlantic Ridge. *J. Sediment. Petrol.*, 43:728–735.

Bonatti, E., Peyve, A., Kepezhinskas, P., Kurentsova, N., Seyler, M., Skolotnev, S., and Udintsev, G., 1992. Upper mantle heterogeneity below the Mid-Atlantic Ridge, 0°–15°N. *J. Geophys. Res.*, 97:4461–4476.

Dick, H.J.B., 1989. Abyssal peridotites, very slow spreading ridges and ocean ridge magmatism. *In* Saunders, A.D., and Norry, M.J. (Eds.), *Magmatism in the Ocean Basins.* Geol. Soc. Spec. Publ. London, 42:71–105.

Dick, H.J.B., and Bullen, T., 1984. Chromian spinel as a petrogenetic indicator in abyssal and alpine-type peridotites and spatially associated lavas. *Contrib. Mineral. Petrol.*, 86:54–76.

Dick, H.J.B., Fisher, R.L., and Bryan, W.B., 1984. Mineralogic variability of the uppermost mantle along mid-ocean ridges. *Earth Planet. Sci. Lett.*, 69:88–106.

Evans, B.W., and Frost, R.F., 1975. Chrome-spinel in progressive metamorphism—a preliminary analysis. *Geochim. Cosmochim. Acta,* 39:957–972.

Francheteau, J., Armijo, R., Cheminée, J.L., Hekinian, R., Lonsdale, P., and Blum, N., 1990. 1 Ma East Pacific Rise oceanic crust and uppermost mantle exposed by rifting in Hess Deep (equatorial Pacific Ocean). *Earth Planet. Sci. Lett.*, 101:281–295.

————, 1992. Dyke complex of the East Pacific Rise exposed in the walls of Hess Deep and the structure of the upper oceanic crust. *Earth Planet. Sci. Lett.*, 111:109–121.

Gillis, K., Mével, C., Allan, J., et al., 1993. *Proc. ODP, Init. Repts.*, 147: College Station, TX (Ocean Drilling Program).

Irvine, T.N., 1967. Chromium spinel as a petrogenetic indicator. Part 2: Petrological applications. *Can. J. Earth Sci.*, 4:71–103.

Jackson, E.D., 1969. Chemical variation in co-existing chromite and olivine in chromite zones of the Stillwater complex. *In* Wilson, H.D.B. (Ed.), *Magmatic Ore Deposits.* Econ. Geol. Monogr., 6:41–71.

Date of initial receipt: 2 August 1994
Date of acceptance: 29 November 1994
Ms 147SR-006

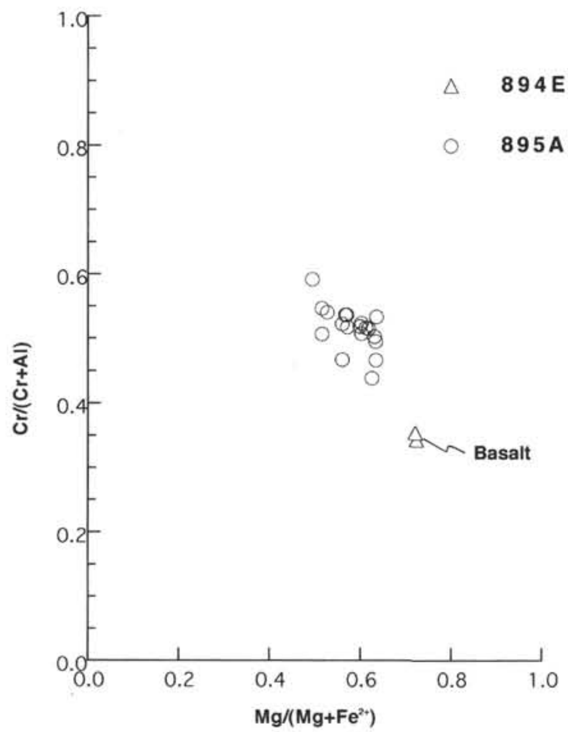

Figure 1. Relationship between the Cr/(Cr + Al) and $Mg/(Mg + Fe^{2+})$ atomic ratios of the detrital chromian spinel from Hess Deep.

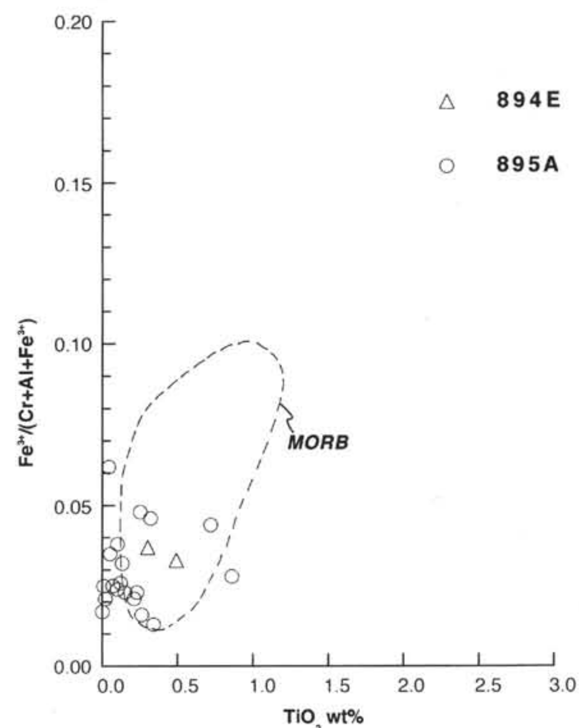

Figure 2. Relationship between the $Fe^{3+}/(Cr + Al + Fe^{3+})$ atomic ratio and TiO_2 content of the detrital chromian spinel from Hess Deep. The MORB field is after Arai (1992).

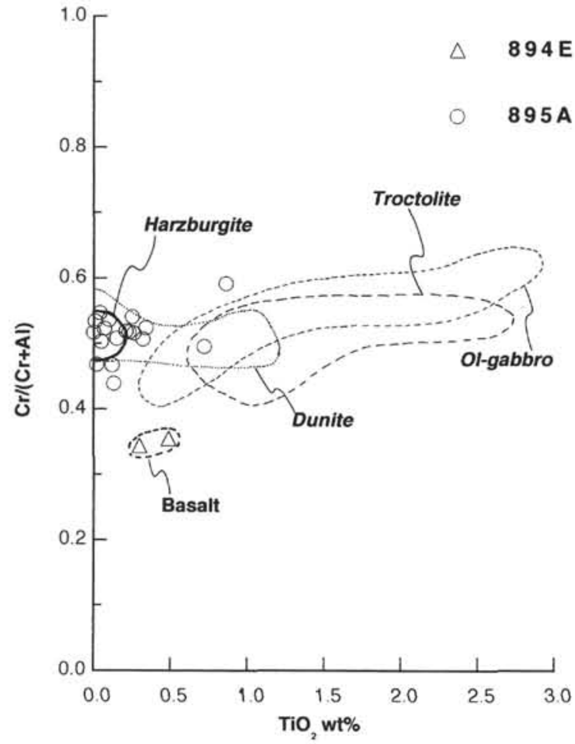

Figure 3. Relationship between the Cr/(Cr + Al) atomic ratio and TiO_2 content of the detrital chromian spinel from Hess Deep. The regions for cored rocks of Site 895 are after Arai and Matsukage (this volume).

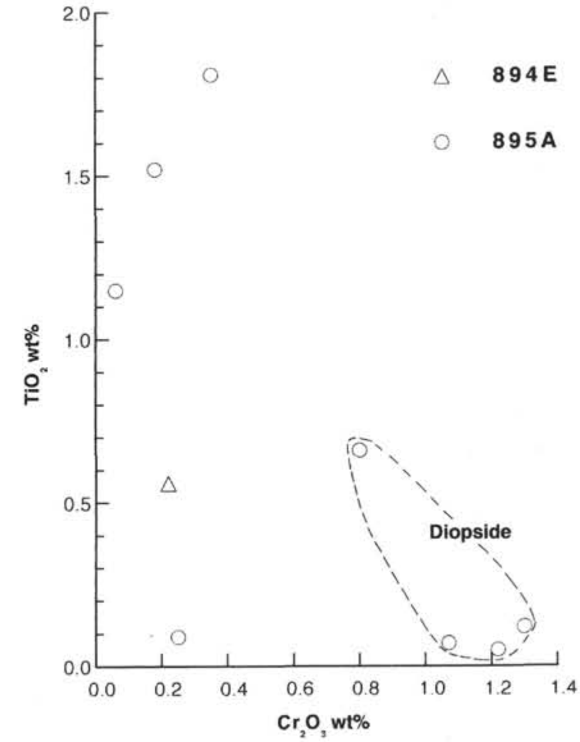

Figure 4. Relationship between the TiO_2 content and Cr# of the detrital clinopyroxenes from Hess Deep.

Table 2. Electron microprobe analyses of the detrital silicate minerals from Hess Deep.

	894D												894E	
	Olivine				Clinopyroxene	Plagioclase					Hornblende		Olivine	
SiO_2	40.32	41.07	41.10	40.20	51.47	67.10	68.39	55.68	55.42	47.23	49.47	49.10	40.69	40.45
TiO_2	0.04	0.13	0.15	0.01	0.56	0.02	0.00	0.12	0.11	0.10	1.27	1.01	0.01	0.07
Al_2O_3	0.33	0.14	0.44	0.40	1.80	20.36	19.86	27.96	28.31	33.19	15.12	15.93	0.36	0.34
Cr_2O_3	0.14	0.15	0.07	0.10	0.22	0.04	0.01	0.05	0.00	0.11	0.14	0.08	0.06	0.16
FeO*	13.15	9.74	9.49	13.51	10.78	0.09	0.13	0.48	0.37	0.37	9.37	8.47	11.25	11.63
MnO	0.26	0.24	0.09	0.26	0.32	0.07	0.05	0.01	0.02	0.11	0.19	0.18	0.15	0.23
MgO	45.55	48.33	48.46	45.07	13.47	0.00	0.00	0.00	0.00	0.17	7.92	8.45	47.16	46.69
CaO	0.42	0.31	0.32	0.46	20.46	1.05	0.19	10.83	10.43	17.21	11.57	12.01	0.31	0.39
Na_2O	0.00	0.00	0.01	0.00	0.33	10.73	11.23	4.52	5.19	1.34	2.21	1.92	0.00	0.00
K_2O	0.01	0.01	0.00	0.06	0.00	0.09	0.00	0.08	0.13	0.00	0.04	0.03	0.00	0.00
NiO	0.18	0.31	0.35	0.21	0.08	0.08	0.05	0.00	0.00	0.00	0.05	0.10	0.30	0.29
Total	100.39	100.42	100.50	100.28	99.49	99.62	99.92	99.72	100.00	99.85	97.35	97.27	100.31	100.25
Mg#	0.861	0.898	0.901	0.856	0.690						0.601	0.640	0.882	0.877
An						5.70	1.90	48.80	50.30	80.30				

Notes: FeO* and Fe* are total iron as FeO and Fe, respectively. Mg# is Mg(Me + Fe*) atomic ratio.

	895A															
	Olivine											Clinopyroxene				
SiO_2	41.17	41.29	41.56	41.31	40.98	41.19	41.40	40.97	40.98	40.90	41.31	50.62	52.85	52.14	49.65	52.15
TiO_2	0.04	0.06	0.00	0.31	0.06	0.00	0.13	0.00	0.00	0.14	0.03	1.15	0.09	0.66	1.52	0.05
Al_2O_3	0.16	0.35	0.36	0.26	0.24	0.14	0.17	0.27	0.30	0.18	0.18	2.00	0.82	2.55	4.28	3.30
Cr_2O_3	0.13	0.00	0.05	0.00	0.00	0.09	0.09	0.00	0.07	0.10	0.00	0.06	0.26	0.80	0.18	1.22
FeO*	9.18	8.87	8.53	8.88	8.56	8.38	8.47	9.21	8.68	8.76	9.10	16.07	8.31	4.00	10.45	2.87
MnO	0.05	0.17	0.17	0.08	0.08	0.17	0.17	0.07	0.16	0.21	0.09	0.46	0.39	0.13	0.21	0.00
MgO	49.16	49.16	49.31	49.19	49.87	49.81	49.59	49.25	49.89	49.68	49.08	12.20	14.04	17.43	16.54	17.75
CaO	0.14	0.12	0.11	0.15	0.10	0.07	0.13	0.10	0.07	0.07	0.15	16.67	22.51	21.61	15.99	21.90
Na_2O	0.00	0.00	0.00	0.00	0.00	0.00	0.00	0.00	0.00	0.00	0.00	0.00	0.00	0.00	0.15	0.00
K_2O	0.01	0.00	0.00	0.00	0.06	0.03	0.00	0.01	0.00	0.00	0.04	0.00	0.03	0.00	0.04	0.00
NiO	0.33	0.49	0.31	0.32	0.47	0.46	0.36	0.56	0.31	0.43	0.36	0.25	0.01	0.09	0.11	0.09
Total	100.37	100.50	100.41	100.50	100.43	100.35	100.50	100.44	100.47	100.48	100.36	99.48	99.31	99.40	99.13	99.33
Mg#	0.905	0.908	0.912	0.908	0.912	0.914	0.913	0.905	0.911	0.910	0.906	0.575	0.751	0.886	0.738	0.917
An																

	895A												
	Clinopyroxene			Orthopyroxene		Plagioclase				Hornblende			
SiO_2	52.65	49.18	52.63	56.22	55.87	62.41	55.28	53.80	53.11	51.72	48.55	50.17	49.06
TiO_2	0.07	1.81	0.12	0.07	0.13	0.04	0.07	0.10	0.24	2.35	1.28	2.19	1.22
Al_2O_3	2.39	4.54	2.53	2.55	2.29	23.03	27.59	28.65	27.63	13.91	16.19	13.74	15.85
Cr_2O_3	1.07	0.35	1.30	0.80	0.77	0.04	0.17	0.11	0.18	0.10	0.13	0.19	0.16
FeO*	2.46	9.35	2.79	5.83	5.68	0.76	1.15	1.12	1.23	12.70	8.66	12.31	8.78
MnO	0.18	0.17	0.04	0.21	0.15	0.03	0.03	0.03	0.11	0.27	0.13	0.11	0.17
MgO	17.49	14.73	17.16	32.28	32.37	0.00	0.26	0.00	0.00	5.68	8.66	6.27	8.32
CaO	22.85	18.93	22.60	2.14	2.92	5.05	10.17	12.07	12.41	10.45	11.61	10.32	11.48
Na_2O	0.00	0.00	0.00	0.00	0.00	8.19	5.13	3.89	4.79	1.56	1.87	1.58	2.28
K_2O	0.00	0.00	0.00	0.03	0.02	0.21	0.05	0.05	0.15	0.22	0.09	0.12	0.01
NiO	0.01	0.09	0.08	0.27	0.09	0.08	0.00	0.01	0.00	0.00	0.00	0.07	0.00
Total	99.17	99.16	99.25	100.39	100.29	99.83	99.90	99.84	99.85	98.96	97.16	97.07	97.33
Mg#	0.927	0.737	0.917	0.908	0.910					0.444	0.641	0.476	0.628
An						21.70	50.00	54.60	53.10				

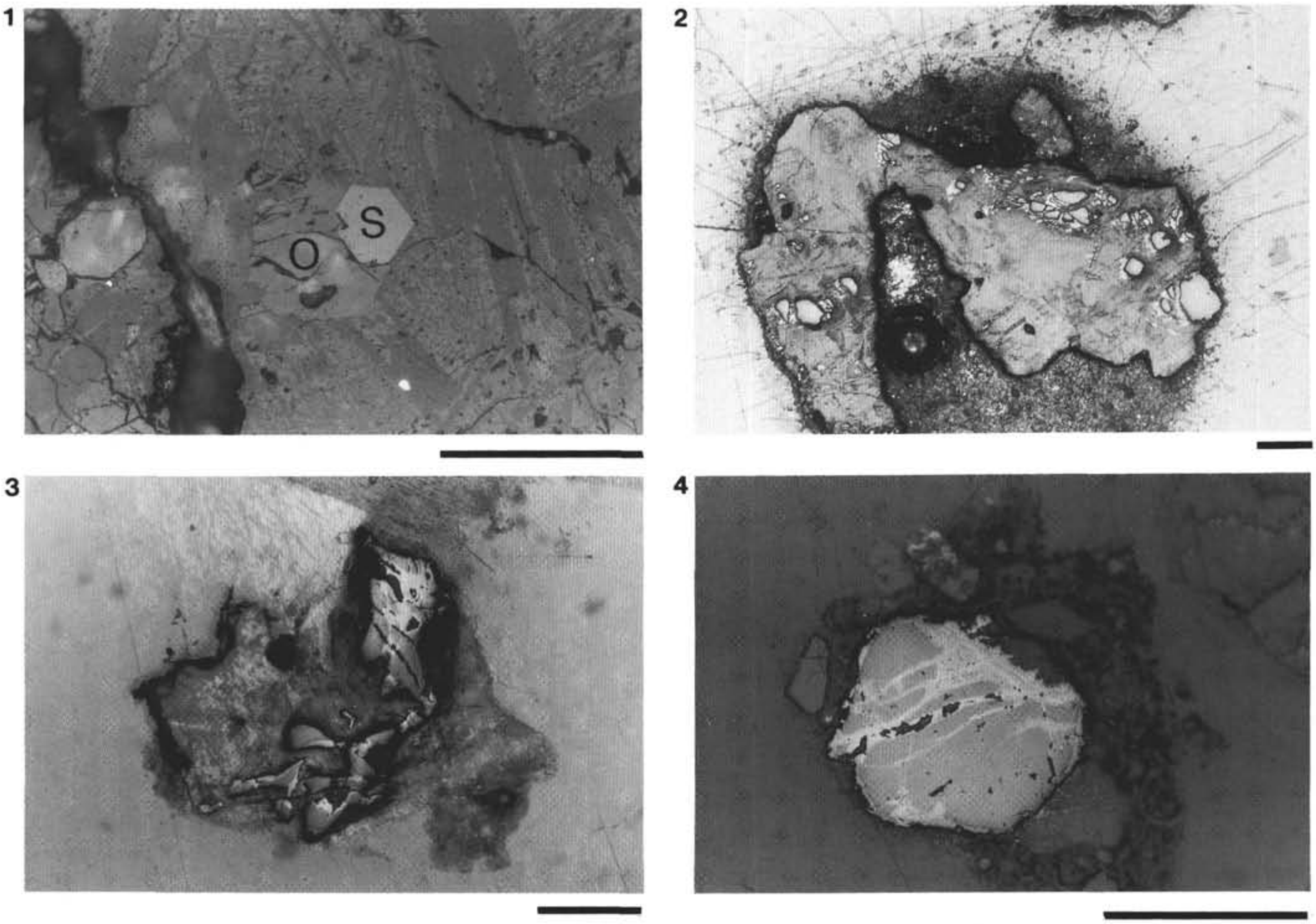

Plate 1. Reflected-light photomicrographs of clastic particles in the surface sediments from Hess Deep. Scale bar is 0.2 mm. **1.** Olivine phenocryst (O) with euhedral spinel (S) in a basalt pebble from Hole 894E. **2.** Subrounded particle of serpentinized peridotite from Hole 895A. The relic olivine has high relief. Note that the original shape of the particle was destroyed during sample processing. **3.** Highly anhedral chromian spinel particle from Hole 895A, possibly derived from harzburgite. **4.** Subhedral chromian spinel particle from Hole 895A, possibly derived from dunite.